J|A|C|S
ARTICLES
Published on Web 03/28/2002

Metal−Benzene and Metal−CO Bond Energies in Neutral and Ionic $C_6H_6Cr(CO)_3$ Studied by Threshold Photoelectron−Photoion Coincidence Spectroscopy and Density Functional Theory

Yue Li,[†] John E. McGrady,[‡] and Tomas Baer*,[†]

Contribution from the Department of Chemistry, University of North Carolina, Chapel Hill, North Carolina 27599-3290 and Department of Chemistry, University of York, Heslington, York YO10 5DD, United Kingdom

Received November 30, 2001

Abstract: Threshold photoelectron−photoion coincidence spectroscopy and density functional theory calculations have been used to investigate the dissociation kinetics of the benzene chromium tricarbonyl ion, $BzCr(CO)_3^+$ ($Bz = C_6H_6$). The dissociation of the $BzCr(CO)_3^+$ ion proceeds by the sequential loss of three CO and benzene ligands. The first and third CO and the benzene loss reactions were associated with metastable precursor ions (lifetimes in the microsecond range). By simulating the resulting asymmetric time-of-flight peak shapes and breakdown diagram, the 0 K appearance energies of the four product ions were determined to be 8.33 ± 0.05, 8.93 ± 0.05, 9.97 ± 0.06, and 11.71 ± 0.06 eV, respectively. Combined with the ionization energy of $BzCr(CO)_3$, 7.30 ± 0.05 eV, the three successive Cr−CO bond energies in the $BzCr(CO)_3^+$ were found to alternate, with values of 1.03 ± 0.05, 0.60 ± 0.05, and 1.04 ± 0.05 eV, respectively, and the Bz−Cr bond energy in $BzCr^+$ is 1.74 ± 0.05 eV, a trend confirmed by the density functional theory (DFT) calculations. Using the heats of formation of the fully dissociated products, C_6H_6, Cr^+, and CO, the 298 K heats of formation the ionic $BzCr(CO)_n^+$ ($n = 0 \rightarrow 3$) species were determined. By scaling the DFT calculated bond energies for the neutral molecules, the heats of formation of the neutral $BzCr(CO)_n$ ($n = 0 \rightarrow 3$) were also obtained.

Introduction

The structures and reactivities of the arene chromium tricarbonyls have been the subject of extensive investigation in organometallic chemistry[1−3] because of the importance of this class of transition metal complexes in catalysis[4] and organic synthesis.[5,6]

Benzene chromium tricarbonyl, $C_6H_6Cr(CO)_3$ or $BzCr(CO)_3$, is the simplest arene chromium tricarbonyl complex, and this molecule has therefore been the object of many theoretical[7−11] and experimental studies.[12−18] The structure of $BzCr(CO)_3$ has been the source of much controversy, in both theoretical and experimental studies. Early room-temperature X-ray diffraction,[19,20] Raman and IR studies[21,22] suggested that the benzene ring in this molecule retained D_{6h} symmetry, but more recent low-temperature X-ray and neutron diffraction studies[23] show that the benzene ring is in fact distorted in the solid state. The gas-phase structure of $BzCr(CO)_3$ was recently determined by microwave spectroscopy by Kukolich et al.,[24−26] who found that

* Corresponding author. E-mail: baer@unc.edu.
[†] University of North Carolina.
[‡] University of York.

(1) Davis, R.; Kane-Maguire, L. A. P. In *Comprehensive Organometallic Chemistry*; Wilkinson, G., Ed.; Pergamon Press: Oxford, U.K., 1982; p 953.
(2) Muetterties, E. L.; Bleeke, J. R.; Wucherer, E. J.; Albright, T. A. *Chem. Rev.* **1982**, *82*, 499−525.
(3) Albright, T. A. *Acc. Chem. Res.* **1982**, *15*, 149−155.
(4) Tsonis, C. P.; Hwang, J. S. *J. Mol. Catal.* **1984**, *26*, 219−229.
(5) Pearson, A. J. In *Metallo-Organic Chemistry*; John Wiley and Sons: New York, 1985.
(6) Jaouen, G. In *Transition Metal Organometallics in Organic Synthesis*; Alper, H., Ed.; Academic: New York, 1978; pp 65−120.
(7) Fitzpatrick, N. J.; Savariault, J. M.; Labarre, J. F. R. *J. Organomet. Chem.* **1977**, *127*, 325−335.
(8) McGrady, J. E.; Dyson, P. J. *J. Organomet. Chem.* **2000**, *607*, 203−207.
(9) Schleyer, P. v. R.; Kiran, B.; Simion, D. V.; Sorensen, T. S. *J. Am. Chem. Soc.* **2000**, *122*, 510−513.
(10) Suresh, C. H.; Koga, N.; Gadre, S. R. *Organometallics* **2000**, *19*, 3008−3015.
(11) Elass, A.; Mahieu, J.; Brocard, J.; Surpateanu, G.; Vergoten, G. *J. Mol. Struct.* **1999**, *475*, 279−286.
(12) Armstrong, R. S.; Aroney, M. J.; Barnes, C. M.; Klepetko, J. A.; Maschmeyer, T.; Masters, A. F.; Niles, D. *J. Mol. Struct.* **1997**, *406*, 219−222.
(13) Armstrong, R. S.; Aroney, M. J.; Barnes, C. M.; Nugent, K. W. *J. Mol. Struct.* **1994**, *323*, 15−28.
(14) Chhor, K.; Lucazeau, G. *J. Raman Spectrosc.* **1982**, *13*, 235−246.
(15) English, A. M.; Plowman, K. R.; Butler, I. S. *Inorg. Chem.* **1982**, *21*, 338−347.
(16) Gilson, D. F. R.; Gomez, G.; Bulter, I. S.; Fitzpatrick, P. J. *Can. J. Chem.* **1983**, *61*, 737−742.
(17) Chhor, K.; Sourisseau, C.; Lucazeau, G. *J. Mol. Struct.* **1982**, *80*, 485−488.
(18) Wittmann, G. T. W.; Krynauw, G. N.; Lotz, S. *J. Organomet. Chem.* **1985**, *293*, C33−C37.
(19) Bailey, M. F.; Dahl, L. F. *Inorg. Chem.* **1965**, *4*, 1298.
(20) Bailey, M. F.; Dahl, L. F. *Inorg. Chem.* **1965**, *4*, 1314.
(21) Brunvoll, J.; Cyvin, S. J.; Schäfer, L. *J. Organomet. Chem.* **1972**, *36*, 143.
(22) Catlaiotti, R.; Poletti, A.; Santucci, A. *J. Mol. Struct.* **1970**, *5*, 215.
(23) Rees, B.; Coppens, P. *Acta Crystallogr.* **1973**, B*29*, 2515−2528.
(24) Kukolich, S. G.; Sickafoose, S. M.; Flores, L. D.; Breckenridge, S. M. *J. Chem. Phys.* **1994**, *100*, 6125−6128.
(25) Sickafoose, S. M.; Breckenridge, S. M.; Kukolich, S. G. *Inorg. Chem.* **1994**, *33*, 5176−5179.
(26) Kukolich, S. G. *J. Am. Chem. Soc.* **1995**, *117*, 5512−5514.

10.1021/ja012630m CCC: $22.00

the symmetry of benzene reduces to C_{3v} due to the interactions with the $Cr(CO)_3$ moiety. Theoretical studies[9,10,27,28] of the benzene and $Cr(CO)_3$ interaction indicate that upon coordination to the strongly electron withdrawing $Cr(CO)_3$, the benzene ring becomes π-depleted and reduced in aromaticity. The properties of the benzene ligand are significantly changed relative to free benzene, as is reflected in the alternating C−C bond lengths.

The first photoelectron spectrum (PES) of $BzCr(CO)_3$ was reported by Guest et al.,[29] who obtained an estimate of 7.42 eV for the vertical ionization energy (IE). Two different values for the adiabatic IE values of $BzCr(CO)_3$ have been obtained (7.3 and 7.41 eV), based on charge-transfer transition energy measurements.[30,31] In several electron ionization studies of $BzCr(CO)_3$,[32−35] the appearance energies (AE) of the molecular ion, $BzCr(CO)_3^+$, and the fragment ions were measured. The $BzCr(CO)_3^+$ ion was found to undergo fragmentation by successive loss of three CO ligands, followed by loss of the coordinated benzene. The electron ionization studies do not, however, lead to accurate ion energetics because of insufficient energy resolution and the neglect of the sample's thermal energy distribution, as well as the kinetic shift in the data analysis.

In this study we report the investigation of the gas-phase dissociation kinetics of $BzCr(CO)_3^+$ ions using threshold photoelectron−photoion coincidence (TPEPICO) spectroscopy, a technique by which the ions can be energy-selected. The analysis of the experimental results with statistical unimolecular reaction theory can extract accurate dissociation energies of the ions, and thus bond energies and heats of formation. By combining these results with density functional theory (DFT), it is possible to determine an accurate and self-consistent set of bond energies for both neutral and ionic $BzCr(CO)_3$.

Experimental Approach

The threshold photoelectron−photoion coincidence apparatus has been described in detail previously.[36] Briefly, sample vapor was leaked into the experimental chamber through a 1.0 mm diameter inlet (2.5 cm long) and was then ionized with vacuum ultraviolet (vacuum-UV) light from an H_2 discharge lamp dispersed by a 1 m normal incidence monochromator. The vacuum-UV wavelengths were calibrated using the hydrogen Lyman-α line. The ions and the electrons were extracted in opposite directions with an electric field of 20 V/cm. Threshold photoelectrons were selected by a steradiancy analyzer that consists of a flight tube with small apertures that stop energetic electrons with perpendicular velocity components. Further discrimination against the energetic electrons was provided by a hemispherical electrostatic sector analyzer, which resulted in a 35 meV combined photon and electron energy resolution. The ions were accelerated to 100 eV in the first 5 cm long acceleration region and were then accelerated to 220 eV in a short second region. The ions were detected after drifting through a 30 cm field-free drift region. The electrons and ions were detected with a channeltron electron multiplier and a multichannel plate detector, respectively. The electron and ion signals served as start and stop pulses for measuring the ion time-of-flight (TOF), and the TOF for each coincidence event was stored in a multichannel pulse height analyzer. TOF distributions were obtained in 1−72 h, depending on the photon intensity and the desired spectrum quality.

The TPEPICO spectra were used for two purposes. First, the fractional abundances of the precursor and the product ions were measured as a function of the photon energy (breakdown diagram). Second, the product ion TOF distributions were measured at energies close to the dissociation limit. Slowly dissociating (metastable) ions decay in the first acceleration region. The resulting product ion TOF distribution is asymmetrically broadened toward long TOF. The asymmetric peak shapes can be analyzed to extract the ion dissociation rates as a function of the ion internal energy. These two types of information were used together in the data analysis.

The benzene chromium tricarbonyl sample ($BzCr(CO)_3$, 98%, Strem Chemicals) was used without further purification.

Determination of the Sample Temperature. It was necessary to heat the solid sample to 130 °C to obtain sufficient vapor pressure. However, this is not the real temperature of the sample vapor in the ionization region because after the sample passes through the 2.5 cm long quartz tube, it will cool. To obtain an estimate of the real sample temperature, a similar organometallic compound, $CpMn(CO)_3$ ($Cp = C_5H_5$), whose breakdown diagram at room temperature has been determined and well-characterized, was used.[37] From an analysis of the $CpMn(CO)_3$ breakdown diagram at a nominal sample cell temperature of 130 °C, it was determined that the real sample temperature under these conditions is only 67 °C. In this analysis all $CpMn(CO)_3$ parameters were kept fixed while only the assumed temperature was varied. This temperature is used in the simulations of the present $BzCr(CO)_3$ data. No $C_6H_6^+$ ions were observed in this study, which indicates that the thermal decomposition of the sample did not occur as a result of heating the sample.

Quantum Chemical Calculations. In the simulations of the experimental data, vibrational frequencies and rotational constants of the equilibrium structures and transition states for relevant neutral and ionic species are required. In this study, these were obtained from quantum chemical calculations performed using either the Amsterdam density functional package (ADF99)[38−41] or Gaussian 98.[42] Structural and energetic results using the ADF package have been reported previously, and the reader is referred to ref 8 for details of the calculation. Calculations using the Gaussian package were performed on various spin states of the neutral and ionic $BzCr(CO)_3$, $BzCr(CO)_2$, BzCrCO, and BzCr structures using the hybrid B3LYP functional. The 6-31G(d) basis set was used for the carbon and oxygen atoms, while the 6-31G basis set was used for hydrogen. The LANL2DZ[43,44] basis set and effective core potential were used for the chromium atom. The

(27) Simion, D. V.; Sorensen, T. S. *J. Am. Chem. Soc.* **1996**, *118*, 7345−7352.
(28) Bérces, A.; Ziegler, T. *J. Phys. Chem.* **1994**, *98*, 13233−13242.
(29) Guest, M. F.; Hiller, I. H.; Higginson, B. R.; Lloyd, D. R. *Mol. Phys.* **1975**, *29*, 113−128.
(30) Huttner, G.; Fischer, E. O. *J. Organomet. Chem.* **1967**, *8*, 299−310.
(31) Kobayashi, H.; Kobayashi, M.; Kaizu, Y. *Bull. Chem. Soc. Jpn.* **1973**, *46*, 3109−3116.
(32) Gaivoronskii, P. E.; Larin, N. V.; Sirotkin, N. I.; Artemov, A. N.; Shushunov, N. V. *Bull. Acad. Sci. USSR, Div. Chem. Sci.* **1973**, *22*, 2557−2559.
(33) Gilbert, J. R.; Leach, W. P.; Miller, J. R. *J. Organomet. Chem.* **1973**, *49*, 219−225.
(34) Müller, J.; Göser, P. *Chem. Ber.* **1969**, *102*, 3314−3323.
(35) Pignataro, S.; Lossing, F. P. *J. Organomet. Chem.* **1967**, *10*, 531−534.
(36) Baer, T.; Booze, J. A.; Weitzel, K. M. Photoelectron photoion coincidence studies of ion dissociation dynamics. In *Vacuum ultraviolet photoionization and photodissociation of molecules and clusters*; Ng, C. Y., Ed.; World Scientific: Singapore, 1991; pp 259−298.
(37) Li, Y.; Sztaray, B.; Baer, T. *J. Am. Chem. Soc.* **2001**, *123*, 9388−9396.
(38) Versluis, L.; Ziegler, T. *J. Chem. Phys.* **1988**, *88*, 322−328.
(39) te Velde, G.; Baerends, E. J. *J. Comput.Chem.* **1992**, *99*, 84−98.
(40) Baerends, E. J.; Ellis, E. J.; Ros, D. E. *Chem. Phys.* **1973**, *2*, 41−51.
(41) Fonseca, G. C.; Snijders, J. G.; te Velde, G.; Baerends, E. J. *Theor. Chem. Acc.* **1988**, *99*, 391−403.
(42) Frisch, M. J.; Trucks, G. W.; Schlegel, H. B.; Scuseria, G. E.; Robb, M. A.; Cheeseman, J. R.; Zakrzewski, V. G.; Montgomery, J. A., Jr.; Stratmann, R. E.; Burant, J. C.; Dapprich, S.; Millam, J. M.; Daniels, A. D.; Kudin, K. N.; Strain, M. C.; Farkas, O.; Tomasi, J.; Barone, V.; Cossi, M.; Cammi, R.; Mennucci, B.; Pomelli, C.; Adamo, C.; Clifford, S.; Ochterski, J.; Petersson, G. A.; Ayala, P. Y.; Cui, Q.; Morokuma, K.; Malick, D. K.; Rabuck, A. D.; Raghavachari, K.; Foresman, J. B.; Cioslowski, J.; Ortiz, J. V.; Stefanov, B. B.; Liu, G.; Liashenko, A.; Piskorz, P.; Komaromi, I.; Gomperts, R.; Martin, R. L.; Fox, D. J.; Keith, T.; Al-Laham, M. A.; Peng, C. Y.; Nanayakkara, A.; Gonzalez, C.; Challacombe, M.; Gill, P. M. W.; Johnson, B. G.; Chen, W.; Wong, M. W.; Andres, J. L.; Head-Gordon, M.; Replogle, E. S.; Pople, J. A. *Gaussian 98*, Revision A.7; Gaussian, Inc.: Pittsburgh, PA, 1998.
(43) Wadt, W. R.; Hay, P. J. *J. Chem. Phys.* **1985**, *82*, 284.
(44) Dunning, T. H., Jr.; Hay, P. J. In *Modern Theoretical Chemistry*; Schaefer, H. F. I., Ed.; Plenum: New York, 1976; pp 1−28.

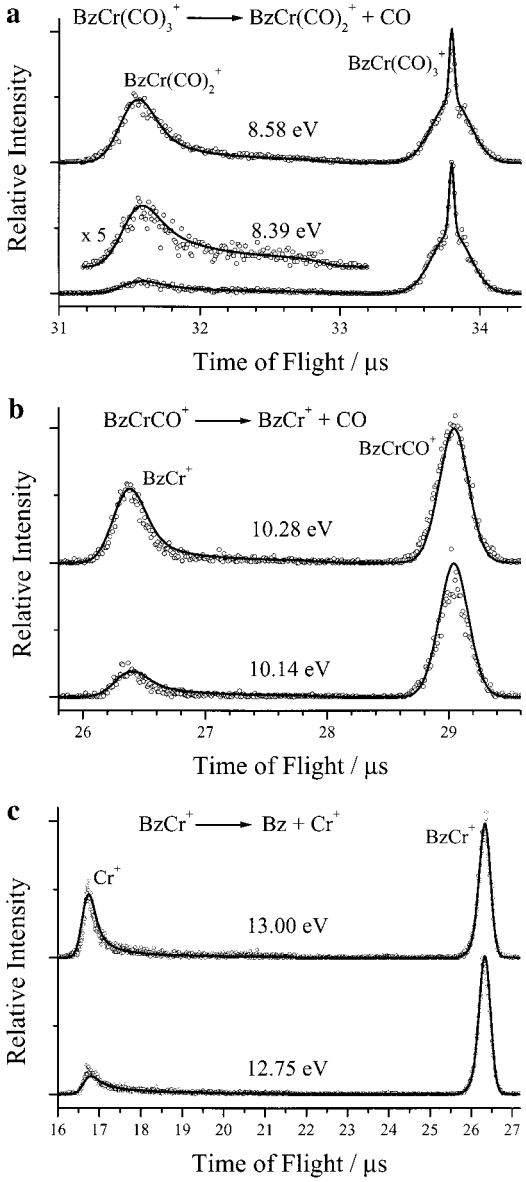

Figure 1. (a, top) Ion TOF distributions at selected photon energies for the first CO loss reaction. The points are the experimental data, and the solid lines are the simulation results. The asymmetric $BzCr(CO)_2^+$ peak at 31.6 μs is due to the slow CO loss reaction. (b, middle) Ion TOF distributions at selected photon energies for the third CO loss reaction. The asymmetric $BzCr^+$ peak at 26.4 μs is due to the slow CO loss reaction. (c, bottom) Ion TOF distributions at selected photon energies for the benzene loss reaction. The asymmetric Cr^+ peak at 16.7 μs is due to the slow benzene loss reaction.

nature of the stationary points was confirmed through the calculation of harmonic vibrational frequencies.

Results and Discussion

1. TOF Distributions and Breakdown Diagram. TOF mass spectra of $BzCr(CO)_3$ were collected in the photon energy range of 7.5→14.2 eV. Typical time-of-flight distributions are shown in Figure 1. The ion peak at 33.8 μs is the molecular ion, $BzCr(CO)_3^+$ (m/z 214), whereas TOF peaks at 31.6, 29.0, 26.4, and 16.7 μs correspond to the product ions, $BzCr(CO)_2^+$ (m/z 186), $BzCrCO^+$ (m/z 158), $BzCr^+$ (m/z 130), and Cr^+ (m/z 52), respectively. In the figures, the points are experimental data and the solid lines are the fitted TOF distributions as discussed in the following section. Figure 1a shows that the precursor

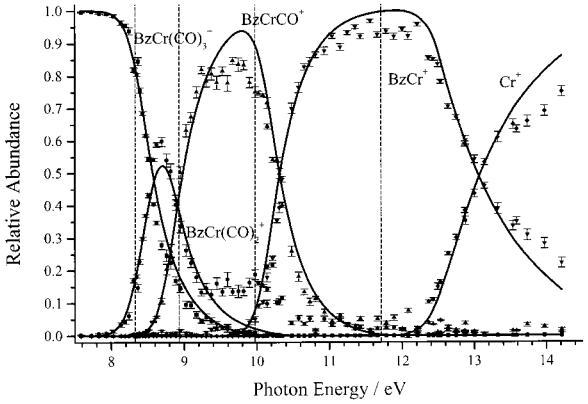

Figure 2. Breakdown diagram of $BzCr(CO)_3^+$. The points are the experimental data with error estimates, and the solid lines are the simulation results. Vertical dashed lines indicate the 0 K appearance energies of the four consecutive dissociation reactions.

ion peak consists of two parts, a central peak on top of a broader one. The sharp part results from the effusive jet produced by the sample inlet, while the broad peak results from the $BzCr(CO)_3$ vapor in the background.

Below a photon energy of 8.4 eV, the two peaks correspond to the molecular ion $BzCr(CO)_3^+$ and its first product ion, $BzCr(CO)_2^+$. At photon energies higher than 8.4 eV, $BzCrCO^+$, the product of double CO loss, can be seen as well. At photon energies in excess of 12.0 eV, the only two peaks correspond to the $BzCr^+$ and Cr^+ ions. The latter ion is a result of the complete dissociative photoionization of the molecular ion to $Cr^+ + C_6H_6 + 3CO$, whose final product energy is well-established. The results are in qualitative agreement with the electron ionization studies that also show these sequential ionization steps.[32,35,45,46]

As shown in Figure 1, for the loss of the first and third carbonyls, as well as of benzene, the product ion TOF distributions are asymmetric at the photon energies close to the appearance energies of those product ions. This indicates that these ions are produced slowly during the course of acceleration in the first acceleration region.

The experimental breakdown diagram of the $BzCr(CO)_3^+$ ion is shown in Figure 2, in which the points are the experimental data with error estimates, the solid lines show the simulation results, and the vertical dashed lines indicate the location of the four 0 K dissociation onsets determined in this study. The crossover energies, in which the abundance of precursor ions and product ions are equal, are 8.6, 8.92, 10.36, and 13.1 eV, respectively.

The dissociation reaction mechanism of the $BzCr(CO)_3^+$ ions can be described by

$$BzCr(CO)_3^+ \xrightarrow{TS_1} BzCr(CO)_2^+ + CO \xrightarrow{TS_2} BzCrCO^+ + 2CO \xrightarrow{TS_3} BzCr^+ + 3CO \xrightarrow{TS_4} Cr^+ + Bz + 3CO \quad (1)$$

In the electron ionization experiments,[32,34,35,45,46] $BzCr(CO)_2^+$ ion is found with low intensity. From the breakdown diagram

(45) Nebrasov, Y. S.; Vasyukova, N. I. *Org. Mass Spectrom.* **1979**, *14*, 422−424.
(46) Vandenheuvel, W. J. A.; Walker, R. W. *J. Organomet. Chem.* **1980**, *190*, 73−82.

in Figure 2, it can be seen that the dissociation onsets of the first and the second CO loss are very close; that is, the $BzCr(CO)_2^+$ ion is stable over only a small energy range and easily dissociates to $BzCrCO^+$ and CO. The poor electron energy resolution in the electron ionization experiments resulted in a very weak $BzCr(CO)_2^+$ signal.

2. Computational Results. The structural parameters (Gaussian 98) for the ground electronic state of each complex are shown in the Supporting Information. The structural and energetic results are very similar to those reported using the ADF package. In particular, there is a distinct trend toward the adoption of higher multiplicity ground states as ligands are progressively lost. Thus, for neutral $BzCr(CO)_n$, the ground-state multiplicities are 1, 3, 3, and 7 for $n = 3$, 2, 1, and 0, respectively, while for the ionic species, $BzCr(CO)_n^+$, the corresponding values are 2, 4, 6, and 6. The ground states of the Cr atom and ion are $^7S_3$ ($3d^54s^1$) and $^6S_{5/2}$ ($3d^5$), respectively, suggesting that the coordination of benzene in isolation is relatively weak and insufficient to induce spin pairing. Similar observations were made for the related organometallic molecule, $CpMn(CO)_3$, where dissociation of the molecular ion (a doublet) produces fragments in nondoublet ground states; i.e., the dissociation proceeds by an adiabatic path.[37] These trends have been interpreted in terms of the reduced effective ligand field in low-coordinate complexes and also the greater gain in exchange energy associated with unpairing electrons in the cation (d^5 configuration). The neutral species $BzCr(CO)_3$ has almost perfect C_{3v} symmetry, with alternating C−C bond lengths, in accord with previous theoretical results.[9,10,27,28] Upon ionization, the major change in the geometry is the lengthening of the Cr−C(O) and Cr−C(benzene) bonds, which extend by an average of nearly 0.07 Å, consistent with the reduced back-bonding in the cation. When CO ligands are lost from the ion, the remaining Cr^+−C(O) and Cr^+−C(benzene) bond lengths are further increased, but this effect is associated with the increase in multiplicity (and therefore occupation of antibonding orbitals), rather than more subtle changes in the magnitude of back-bonding. The symmetries of the $Cr(CO)_n$ moiety in $BzCr(CO)_n^+$ ($n = 2 \rightarrow 1$) are close to C_{2v} and $C_{\infty v}$, respectively, and the symmetry axes are coincident with the approximate C_6 axis of the benzene ring in each case.

The dissociation steps of $BzCr(CO)_3^+$ ions involving the loss of CO or benzene are expected to be direct dissociation reactions without reverse activation barriers. The determination of the structures or the frequencies for these transition states should use variational transition-state theory (VTST),[47−49] in which the transition-state structure varies with the ion energy. However, to simplify the calculation, we assumed a fixed TS geometry as is done in RRKM theory. The precursor ion frequencies were used as estimates for the transition-state frequencies. The Cr−CO stretch modes obtained from the calculations (389, 381, and 340 cm^{-1}) for $BzCr(CO)_n^+$ ($n = 3 \rightarrow 1$, respectively) were assigned as the critical frequencies for the transition states, TS_n ($n = 1 \rightarrow 3$), while the 180 cm^{-1} mode in $BzCr^+$ was used as the critical frequency for the final dissociation step. Four low-frequency modes (other than the benzene ring rotational mode), which ultimately end up as product rotational degrees of freedom, were adjusted to fit the rate data. All the frequencies used in the best simulation are shown in Table S1 in the Supporting Information.

3. Simulations of the Experimental Data. The statistical RRKM theory was used to calculate rate constants of the unimolecular dissociation reactions of the $BzCr(CO)_3^+$ ion shown in eq 1. The RRKM calculations were performed using the formula[47]

$$k(E) = \frac{\sigma N^{\ddagger}(E - E_0)}{h\rho(E)} \tag{2}$$

in which σ is the symmetry parameter, E_0 is the activation energy, $N^{\ddagger}(E - E_0)$ is the sum of states of the transition state from 0 to $E - E_0$, and $\rho(E)$ is the density of states of the ion measured from the bottom of the ion ground-state potential well. The symmetry parameters for $BzCrCO^+$ and $BzCr^+$ are both 1. According to the DFT calculations, the symmetries of $Cr(CO)_n^+$ ($n = 3$ and 2) in $BzCr(CO)_n^+$ are nearly C_{3v} and C_{2v}, respectively. However, for their corresponding transition states the symmetry is reduced to C_s because they have an extended Cr−C(O) bond length. As will be discussed shortly, the benzene ring in these two ions can rotate freely due to a low-energy barrier. Thus, the symmetry parameters for $BzCr(CO)_3^+$ and $BzCr(CO)_2^+$ used in eq 2 are 3 and 2, respectively.

In the electron diffraction studies, Chiu et al.[50] found that the $BzCr(CO)_3$ vapor consists of a mixture of several conformations which differ by the rotational arrangement of the six-membered ring with respect to the carbonyl groups. They concluded that the $BzCr(CO)_3$ molecule in the gas phase is a nearly unhindered rotor. Extended Hückel calculations gave a theoretical estimate of only 1.3 kJ/mol for this rotational barrier,[51] which compares well with an average of 1.9 kJ/mol (based on different levels of theory) reported more recently by Low and Hall,[52] as well as an upper limit of 1.6 kJ/mol obtained from microwave work.[24] Thus, in the calculations of the thermal energy distribution of the molecule and the rate constants in eq 2, this lowest frequency of $BzCr(CO)_3$ was treated as a rotation. From the frequency analysis, the lowest frequencies of $BzCr(CO)_3^+$ and $BzCr(CO)_2^+$ were also assigned as the internal rotation of the benzene ring. The calculated rotational barrier height of 1.9 kJ/mol was used for neutral $BzCr(CO)_3$, as well as for ionic $BzCr(CO)_3^+$ and $BzCr(CO)_2^+$.

Although the TPEPICO resolution is only about 35 meV, the average thermal energy of $BzCr(CO)_3$ is 280 meV (based on the DFT vibrational frequency calculation). To fit the experimental data, it is necessary to interpret the rate constants in terms of a thermal energy distribution. The procedure, described in detail by Sztáray and Baer,[53] involves convolution of the thermal energy distribution of the molecule with the electron analyzer function and the rate constants, $k(E)$ for the four dissociation channels. The electron analyzer function was measured from the threshold photoelectron spectra (TPES) of rare gases, NO or acetylene, which have widely spaced energy levels. However, as discussed by Li et al.,[37] some adjustment of this function is necessary in certain cases. For the further

(47) Baer, T.; Hase, W. L. *Unimolecular Reaction Dynamics: Theory and Experiments*; Oxford University Press: New York, 1996.
(48) Wardlaw, D. M.; Marcus, R. A. *Adv. Chem. Phys.* **1988**, *70*, 231−263.
(49) Hase, W. L. *Chem. Phys. Lett.* **1987**, *139*, 389−394.
(50) Chiu, N. S.; Schäfer, L. *J. Organomet. Chem.* **1975**, *101*, 331−346.
(51) Albright, T. A.; Hofmann, P.; Hofmann, R. *J. Am. Chem. Soc.* **1977**, *99*, 7546.
(52) Low, A. A.; Hall, M. B. *Int. J. Quantum Chem.* **2000**, *77*, 152−160.
(53) Sztaray, B.; Baer, T. *J. Am. Chem. Soc.* **2000**, *122*, 9219−9226.

dissociations of the product ions, $BzCr(CO)_2^+$, $BzCrCO^+$, and $BzCr^+$, their energy distributions were calculated using the Klots equation,[54] by a method described by Sztáray and Baer.[53]

The ion TOF distributions and the breakdown diagram can be calculated using the following information: the thermal energy distribution of the precursor molecule, the acceleration electric fields and the acceleration and drift field lengths, and the adiabatic IE value of $BzCr(CO)_3$. However, in contrast to the vertical IE value,[29] which is well-determined to be 7.42 eV by the PES measurement, the adiabatic IE of $BzCr(CO)_3$ is not well-established. The vertical result should be the upper limit of the adiabatic IE. Two independent charge-transfer studies[30,31] suggest 7.3 and 7.41 eV. We have chosen to use the lower figure of 7.3 eV as the adiabatic ionization energy of the $BzCr(CO)_3$ molecule in the simulation. Given the significant geometry changes (see the Supporting Information) when $BzCr(CO)_3$ is ionized, one expects a significant difference between the vertical and adiabatic IEs. In addition, the lower IE value agrees better with the derived CO loss bond energy. By adjusting the four dissociation limits, the lowest four TS vibrational frequencies (two for TS_4) which determine the entropies of activation (not including the frequency associated with the benzene ring rotation for $BzCr(CO)_3^+$ and $BzCr(CO)_2^+$, because it has been treated as an internal rotation), and to a limited extent the threshold electron analyzer function, the breakdown diagram and the TOF distributions can be simultaneously fitted.

To aid convergence of the optimization procedure, the simulation was carried out in a stepwise fashion. First, the breakdown diagram was modified by summing all product ions. By simulating this breakdown diagram and the TOF distributions for the $BzCr(CO)_2^+$ ion, the energy barrier height (E_1), the transition-state frequencies for the first dissociation reaction, as well as the threshold electron analyzer function, can be determined. Similarly, for the second CO loss reaction, the breakdown diagram was modified by combining the $BzCrCO^+$, $BzCr^+$, and Cr^+ ions. In this fitting, E_1, the transition-state frequencies of the first CO loss reaction and the threshold electron analyzer function, which are obtained in the first simulation, were fixed. Only the energy barrier height (E_2) and the TS_2 frequencies were adjusted until the breakdown diagram and TOF distributions were simultaneously fitted. In a similar manner, the data set with E_1, E_2 and TS_1, TS_2 frequencies fixed was used in the simulation to obtain E_3, E_4 and the TS_3, TS_4 frequencies.

The best fit to the TOF distributions and the breakdown diagram was obtained with the following parameters: $E_1 = 1.03$ eV, $E_2 = 0.60$ eV, $E_3 = 1.04$ eV, and $E_4 = 1.74$ eV. These values are based on the assumed adiabatic ionization energy of 7.30 ± 0.05 eV. The corresponding 0 K appearance energies are 8.33 ± 0.05, 8.93 ± 0.05, 9.97 ± 0.06, and 11.71 ± 0.06 eV, for the $BzCr(CO)_2^+$, $BzCrCO^+$, $BzCr^+$, and Cr^+ ions, respectively. The simulated TOF distributions and breakdown diagram are shown in Figures 1 and 2, and the RRKM calculated rate constant curves are shown in Figure 3. Although the adiabatic ionization energy of $BzCr(CO)_3$ has associated with it an error ± 0.05 eV, the derived appearance energies for the various product channels did not change substantially as the assumed ionization energy was varied. That is, if the IE was raised, the AEs were lowered by corresponding amounts. This

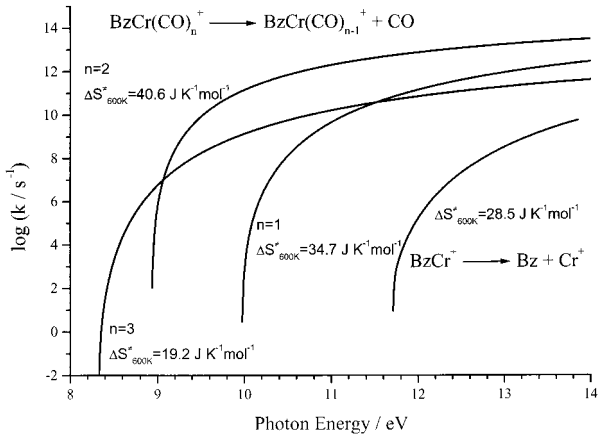

Figure 3. RRKM calculated dissociation rate curves of $BzCr(CO)_3^+$.

is especially true for the higher appearance energies. Any shift of the appearance energies beyond 0.05 eV makes the quality of the simulated TOF distributions and breakdown diagram become significantly worse. We also varied the assumed internal rotational barrier of the benzene ring by multiplying it by a factor of 50→200%, adjusted the sample temperature from 330 to 350 K, and found that all these tests resulted in barrier heights that agreed with the original one within 0.01 eV. These tests led to the estimated error limits of the four appearance energies listed in the above.

The activation entropies of the four consecutive dissociation reactions of 19.2, 40.6, 34.7, and 28.5 $J \cdot mol^{-1} \cdot K^{-1}$ at 600 K, respectively (as shown in Figure 3), are all positive, which indicates that these reactions proceed via loose transition states. This is characteristic of a simple bond-breaking reaction. The 0 K dissociation onsets of the first and third CO loss and the benzene loss steps are 0.27, 0.39, and 1.39 eV lower than their phenomenological crossover energies, respectively, while the second dissociation onset is almost equal to its crossover energy. Because the second CO loss reaction has the highest activation entropy and the lowest bond energy, the dissociation rate constant at the thermochemical onset is quite high so that this onset is not shifted to higher energies as much as the other CO loss onsets.

Table 1 lists experimental dissociation energies and calculated bond energies by two methods determined in this study, and some literature results for comparison. Many of the literature values for the $BzCr(CO)_n^+$ dissociation energies are based on electron ionization appearance energy measurements. These are low-energy resolution studies that did not take into account the thermal energy distribution of the sample nor the kinetic shift in the analysis of experimental data. However, the $Bz-Cr^+$ bond energy of 1.76 ± 0.10 eV obtained by collision induced dissociation[55] agrees very well with our experimental value of 1.74 ± 0.05 eV, as well as with a theoretical calculation of 1.62 ± 0.22 eV obtained using a modified coupled-pair functional method.[56] Table 1 also lists our calculated values based on two density functional approaches. Both computational approaches are conspicuously successful in predicting the trend

(54) Klots, C. E. *J. Chem. Phys.* **1973**, *58*, 5364−5367.

(55) Meyer, F.; Khan, F. A.; Armentrout, P. B. *J. Am. Chem. Soc.* **1995**, *117*, 9740−9748.

(56) Bauschlicher, C. W., Jr.; Partridge, H.; Langhoff, S. R. *J. Phys. Chem.* **1992**, *96*, 3273−3278.

(57) Rosenstock, H. M.; Draxl, K.; Steiner, B. W.; Herron, J. T. *Energetics of gaseous ions*; *Journal of Physical and Chemical Reference Data, Vol. 6;* American Chemical Society: Washington, D.C., 1977.

Table 1. Experimental and Calculated Dissociation Energies (eV)

reactions	this study	calcd[a]	calcd[b]	other
$BzCr(CO)_3^+ \rightarrow BzCr(CO)_2^+ + CO$	1.03	1.19	0.81	0.6,[c] 0.51,[d] 0.4,[e] 1.14[f]
$BzCr(CO)_2^+ \rightarrow BzCrCO^+ + CO$	0.60	0.75	0.28	0.6,[c] 0.84,[d] 0.5[e]
$BzCrCO^+ \rightarrow BzCr^+ + CO$	1.04	1.29	1.20	2.0,[c] 2.25,[d] 1.1[e]
$BzCr^+ \rightarrow Bz + Cr^+$	1.74	2.19	1.68	2.4,[c] 3.16,[d] 3.2,[e] 1.76,[g] 1.62[h]
$BzCr(CO)_3 \rightarrow BzCr(CO)_2 + CO$	2.25[i]	2.08	1.75	
$BzCr(CO)_2 \rightarrow BzCrCO + CO$	2.31[i]	1.91	1.80	
$BzCrCO \rightarrow BzCr + CO$	0.28[i]	1.28[j]	0.22	
$BzCr \rightarrow Bz + Cr$	0.10	0.19[j]	0.10	

[a] DFT results (ADF) (values taken from ref 8 and corrected for ZPE using frequencies reported in Table S1 of the Supporting Information).[b] DFT results (Gaussian 98). [c] Müller and Göser:[34] the values for the first and second CO loss are the average of the two bond energies. [d] Gilbert et al.[33] [e] Gaivoronskii et al.[32] [f] Pignataro and Lossing:[35] the average of the three Cr−C(O) bond energies [g] Meyer et al.[55] [h] Bauschlicher et al.[56] [i] Scaled Gaussian 98 DFT results (see the text). [j] In ref 8, the ground state of BzCr was erroneously reported to be a quintet with an η^6-coordinated benzene ligand. Further investigations carried out as part of this study revealed that a septet, with a weakly η^2-coordinated benzene, is more stable.

in the ionic $BzCr^+$−CO bond energies, the first and third CO loss energies being similar to, and substantially higher than, the second CO loss energy. As previously mentioned, the measured CO loss appearance energy depends only weakly on the assumed $BzCr(CO)_3$ ionization energy. However, the derived bond energy for the loss of the first CO group from $BzCr(CO)_3^+$ depends strongly on the assumed IE. The good correlation with the trends in the calculated and our measured bond energies when we assume an IE of 7.30 eV thus lends support for choosing this value over the 7.41 eV.

4. $BzCr(CO)_3$ and $BzCr(CO)_3^+$ Thermochemistry. The analysis of the experimental TPEPICO results determined all four dissociation energies of $BzCr(CO)_3^+$ to the fully dissociated products, Bz, Cr^+, and CO. Since the heats of formation of Bz, Cr^+, and CO are all well-known, the heats of formation of $BzCr(CO)_n^+$ ($n = 3 \rightarrow 0$) can be accurately determined. For example, the 0 K heat of formation of $BzCr^+$ was obtained using the equation

$$\Delta_f H^o_{0K}[BzCr^+] = \Delta_f H^o_{0K}[Bz] + \Delta_f H^o_{0K}[Cr^+] - [AE(Cr^+) - AE(BzCr^+)] \quad (3)$$

The interconversion between the 0 and 298 K values is performed for neutral or ionic $BzCr(CO)_n$ ($n = 3 \rightarrow 0$) using the following equation:

$$\Delta_f H^o_{298K}[BzCr(CO)_n] = \Delta_f H^o_{0K}[BzCr(CO)_n] - [H^o_{298K} - H^o_{0K}](\text{elements}) + [H^o_{298K} - H^o_{0K}][BzCr(CO)_n] \quad (4)$$

in which "elements" refers to the sum of the elements in their standard states. The $[H^o_{298K} - H^o_{0K}][BzCr(CO)_n]$ value is obtained from the DFT calculated vibrational frequencies. Table 2 lists the 0 and 298 K heats of formation of the relevant species obtained in this study.

The only derived heat of formation that we can compare to a literature value is the $\Delta_f H°$ of the neutral starting compound, $BzCr(CO)_3$. Our 298 K value of -341.5 ± 6 kJ/mol agrees well with the value listed in the Webbook,[58] -350.3 ± 9.4 kJ/mol, which is determined from the microcalorimetric measurements of high-temperature heats of thermal decomposition and of iodination.[61]

Table 2. Thermochemical Data (kJ/mol)[a]

species	$\Delta_f H^o_{298K}$[b]	$\Delta_f H^o_{0K}$[c]	$H^o_{298K} - H^o_{0K}$[d]
$BzCr(CO)_3$	-341.5 ± 6.0	-322.8 ± 6.0[e]	33.28
$BzCr(CO)_2$	-9 ± 15	8 ± 15	29.25
BzCrCO	328 ± 15	345 ± 15	24.17
BzCr	470.9 ± 6.3	485.6 ± 6.3	21.11
$BzCr(CO)_3^+$	365.1 ± 7.7	381.6 ± 7.7	35.44
$BzCr(CO)_2^+$	579.3 ± 7.7	594.8 ± 7.7	30.99
$BzCrCO^+$	752.6 ± 7.0	766.5 ± 7.0	27.24
$BzCr^+$	964.7 ± 5.0	980.6 ± 5.0	19.90
Bz	82.93 ± 0.50[f]	100.33 ± 0.50[g]	8.11
Cr	397.48 ± 4.2[h]	395.34 ± 4.2[h]	−
Cr^+	1050.28 ± 1.5[i]	1048.14 ± 1.5[h]	−
CO	-110.53[j]	-113.80[j]	8.665[j]

[a] In the $H^o_{298K} - H^o_{0K}$ calculations, the heat capacity of the electron was treated as 0.0 kJ/mol at all temperatures (the ion convention[57]). To convert to the electron convention, which treats the electron as a real particle, 6.197 kJ/mol should be added to the 298 K heat of formation of each ion. [b] $\Delta_f H^o_{0K} \rightarrow \Delta_f H^o_{298K}$. [c] Determined using the appearance energies determined in this study. [d] Determined using DFT or HF calculated vibrational frequencies. [e] $\Delta_f H^o_{0K}(Bz) + \Delta_f H^o_{0K}(Cr^+) + 3\Delta_f H^o_{0K}(CO) - AE_{0K}(Cr^+)$. [f] Webbook.[58] [g] $\Delta_f H^o_{298K} \rightarrow \Delta_f H^o_{0K}$. [h] NIST-JANAF thermochemical tables.[59] [i] NIST-JANAF thermochemical tables,[59] converted to the ion convention. [j] Wagman et al.[60]

Having verified the heat of formation of neutral $BzCr(CO)_3$, and knowing the energies of the dissociated products, Bz, Cr, and CO, we can determine the sum of the bond energies in the neutral compound with the equation

$$BzCr(CO)_3(g) \rightarrow C_6H_6(g) + Cr(g) + 3CO(g) \qquad \Delta_r H^o_{0K} = 477 \text{ kJ/mol (4.94 eV)} \quad (5)$$

The corresponding bond energy sum for the ion is

$$BzCr(CO)_3^+(g) \rightarrow C_6H_6(g) + Cr^+(g) + 3CO(g) \qquad \Delta_r H^o_{0K} = 426 \text{ kJ/mol (4.41 eV)} \quad (6)$$

The sum of the Cr−ligand bond energies of the neutral is slightly higher than that of the ion, a direct consequence of the weaker back-bonding and longer Cr−C bonds in the charged species. A recent measurement of the BzCr ionization energy of 5.13 ± 0.04 eV[62] combined with our 0 K heat of formation of $BzCr^+ + 3CO$ (639.2 kJ/mol) fixes the heat of formation of the BzCr + 3CO product at 144.2 kJ/mol. This information allows us to fix the experimental sum of the three BzCr−CO bonds at 4.84 eV and the Bz−Cr bond energy at 0.10 ± 0.06 eV. Since the heat of formation and the IE value of the chromium atom are well-known, using the above sum of the dissociation energies of neutral $BzCrCO_n$ ($n = 3 \rightarrow 0$), the full ionization−dissociation energy diagram of the $BzCr(CO)_3$ system can be established as shown in Figure 4, in which the values are 0 K heats of formation.

(58) http://webbook.nist.gov/chemistry/om/. 2000.

(59) Chase, M. W. *NIST-JANAF Thermochemical Tables*; American Institute of Physics: New York, 1998.

(60) Wagman, D. D.; Evans, W. H. E.; Parker, V. B.; Schum, R. H.; Halow, I.; Mailey, S. M.; Churney, K. L.; Nuttall, R. L. *The NBS Tables of Chemical Thermodynamic Properties*; *Journal of Physical and Chemical Reference Data*; NSRDS: U.S. Government Printing Office: Washington, D.C., 1982; Vol. 11, Suppl. 2.

(61) Pilcher, G.; Skinner, H. A. Thermochemistry of organometallic compounds. In *The Chemistry of the Metal−Carbon Bond*; Hartley, F. R., Patai, S., Eds.; John Wiley & Sons: New York, 1982; pp 43−90.

(62) Kurikawa, T.; Takeda, H.; Hirano, M.; Judai, K.; Arita, T.; Nagao, S.; Nakajima, A.; Kaya, K. *Organometallics* **1999**, *18*, 1430−1438.

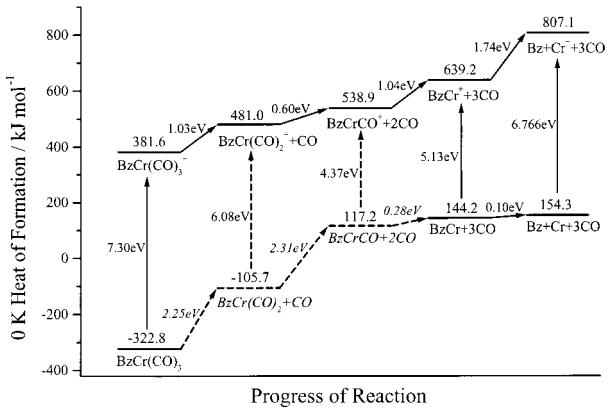

Figure 4. Diagram of heats of formation at 0 K for the ionization and dissociation of the $BzCr(CO)_3$ system. The solid lines and arrows show the experimentally determined energies, while the dashed lines and arrows are the results based on the DFT calculations. The ionization energies of $BzCr(CO)_2$ and BzCrCO are the energy differences between the ions and the neutral.

The experimental values in Table 1 and Figure 4 can now be compared to the calculated bond energies that are listed in Table 1. As noted above, only the sum of the three Cr−CO bond energies (4.84 eV) is known experimentally, and the calculated values of this sum differ widely (5.27 and 3.77 eV for the ADF and Gaussian 98 DFT calculations, respectively). This discrepancy can be traced to the well-known tendency of pure DFT methods (such as BP86[63,64] used in the ADF program) to overestimate the stability of d^ns^0 configurations relative to $d^{n-1}s^1$.[65] Thus, the relative underestimation of the stability of the ^7S ground state of the Cr atom (d^5s^1) by the BP86 functional leads to a larger overall value for the sum of the three dissociation energies. In the cationic species, the much closer agreement between experiment and theory is simply a consequence of the fact the 4s orbital remains unpopulated throughout the reaction sequence. The bias toward d^ns^0 configurations in BP86 is clearly reflected in the prediction of a triplet, rather than septet (B3LYP), ground state for BzCrCO. Given the general consensus that hybrid functionals perform better in describing relative energies of different spin states,[66,67] we choose to employ the individual bond dissociation energies generated by the Gaussian 98 package, rather than those from ADF. By scaling the Gaussian 98 calculations by a factor of 4.84/3.77, we therefore obtain separate estimates of the first, second, and third CO dissociation energies for the neutral species (first column of Table 1 and Figure 4).

We are now faced with an interesting fact. Multiphoton dissociation experiments on neutral $BzCr(CO)_3$ molecules[68−71] have shown that the molecule breaks apart through the loss of CO, rather than Bz. This indicates that the Bz−Cr bond is stronger than the Cr−CO bond, or at least that the activation energy for Bz loss is greater than that for CO loss. In agreement with this, Mukerjee et al.[72] on the basis of solution thermochemical measurements have found that the $Bz-Cr(CO)_3$ bond energy is about 2.3 eV, which is equal to or higher than the neutral Cr−CO bond energies. Yet, both the calculated and the experimental Bz−Cr bond energies shown in Table 1 and Figure 4 indicate that this value in BzCr is about 0.10 eV, far smaller than the Cr−CO bond energies. It is evident that the Bz−Cr bond energy is strongly influenced by the presence of the CO groups. In other words, the presence of the CO groups increases the bond energy between the benzene ring and the Cr atom. Such a drastic change should be reflected in the Bz−Cr bond distances as CO ligands are sequentially lost.

Table 3. Bz−Cr and Cr−CO Bond Lengths and Bond Energies (BE)

	neutral BE (eV)	neutral bond distance (Å)	ion BE (eV)	ion bond distance (Å)
$Bz-Cr(CO)_3$	2.3[a]	1.764	1.86[b]	1.872
$Bz-Cr(CO)_2$		1.744		2.005
Bz−CrCO		1.699		2.196
Bz−Cr	0.10	3.175	1.74	2.216
$BzCr(CO)_2$–CO	2.25	1.847	1.03	1.918
BzCrCO−CO	2.31	1.892	0.60	1.970
BzCr−CO	0.28	1.877	1.04	2.098

[a] Mukerjee et al.[72] [b] Derived from our data and the data of Das et al.[73]

Table 3 lists the experimental and theoretical bond energies along with the calculated distances between the Cr atom and the plane of the benzene molecule or carbonyls. It is apparent that the much weakened Bz−Cr bond is reflected in a much longer Bz−Cr bond distance. Why should the bond energy in the neutral BzCr be so much weaker than in the ionic form? In the septet ground state of the neutral Cr aom, all six valence orbitals (3d + 4s) are singly occupied. As a result, donation of one or more pairs of electrons from the benzene can only occur at the expense of pairing electrons, a relatively unfavorable process in Cr where the 3d orbitals are rather small. The BzCr complex is, in fact, best viewed as a weak van der Waals complex rather than a covalently bonded one. In contrast, the 4s orbital is vacant in the ground state of the Cr^+ ion, and this orbital can act as an electron pair acceptor without significantly increased electron−electron repulsion. This charge transfer, in addition to the inherently larger charge−dipole interaction, leads to the very low observed (and calculated) Bz−Cr bond energy. Similar arguments can be put forward to rationalize the marked difference between BP86- and B3LYP-calculated CO dissociation energies in BzCrCO, the only point where a major discrepancy between the two theoretical techniques was observed. The B3LYP calculation predicts a triplet ground state for BzCrCO, leading to a low dissociation energy for the reasons noted above. The BP86 functional, however, predicts a septet ground state for BzCrCO, and hence a much stronger Cr−CO bond.

In contrast to the Bz−Cr bond energies, which are inversely related to the bond length, the Cr−CO bond energies show no direct correlation with bond length (1.918, 1.970, and 2.098 Å for $n = 3$, 2, and 1, respectively) contrary to the suggestion of

(63) Perdew, J. P. *Phys. Rev. B* **1986**, *33*, 8822−8824.
(64) Becke, A. D. *Phys. Rev. A* **1988**, *38*, 3098−3100.
(65) Russo, T. V.; Martin, R. L.; Hay, P. J. *J. Chem. Phys.* **1994**, *101*, 7729−7737.
(66) Ricca, A.; Bauschlicher, C. W., Jr. *J. Phys. Chem.* **1994**, *98*, 12899−12903.
(67) González-Blanco, O.; Branchadell, V. *J. Chem. Phys.* **1999**, *110*, 778−783.
(68) Wang, W. H.; Jin P.; Liu, Y. W.; She, Y. b.; Fu, K. J. *J. Phys. Chem.* **1992**, *96*, 1278−1283.
(69) Fisanick, G. J.; Gedanken, A.; Eichelberger, T. S. I.; Kuebler, N. A.; Robin, M. B. *J. Chem. Phys.* **1981**, *75*, 5215−5225.
(70) Opitz, J.; Bruch, D.; Bünau, G. *Int. J. Mass Spectrom. Ion. Processes* **1993**, *125*, 215−228.
(71) Dale, M. J.; Dyson, P. J.; Suman, P.; Zenobi, R. *Organometallics* **1997**, *16*, 197−204.
(72) Mukerjee, S. L.; Lang, R. F.; Ju, T.; Kiss, G.; Hoff, C. D.; Nolan, S. P. *Inorg. Chem.* **1992**, *31*, 4885−4889.
(73) Das, P. R.; Nishimura, T.; Meisels, G. G. *J. Phys. Chem.* **1985**, *89*, 2808−2812.

Calhorda et al.[74] that the bond energies should weaken progressively as the number of CO groups is reduced. The origin of this apparent paradox is simply that a direct correlation between bond length and strength can only be expected where there is no change in multiplicity in the course of the reaction. If such a change does take place, it serves both to reduce the bond strength (as noted in ref 8) and to increase the bond length in the ligand deficient species, by populating antibonding orbitals. Thus, more generally, we might anticipate an inverse correlation between bond energy and change in bond length (rather than bond length itself), and such a trend is indeed apparent in Table 3. The excellent correlation between bond length and bond strength in BzCr and $BzCr^+$ is simply a consequence of the fact that no change in multiplicity occurs upon dissociation of the ligand.

Mukerjee et al.[72] measured the neutral $Bz-Cr(CO)_3$ bond energy. Although the ionic $Bz-Cr(CO)_3^+$ bond energy has not been directly measured, we can derive it from the known thermochemistry of the molecules and ions in the following reaction:

$$BzCr(CO)_3^+ \rightarrow Cr(CO)_3^+ + Bz \qquad (7)$$

The heat of formation of the $Cr(CO)_3^+$ ion can be derived from a previous TPEPICO study of Das et al.[73] and the photoionization mass spectrometric study of Chen et al.,[75] in which the appearance energies of the various $Cr(CO)_n^+$ ($n = 6\rightarrow0$) were determined by photoionization of $Cr(CO)_6$. If we use the reasonably well-established 298 K heat of formation of the $Cr(CO)_6$ complex of -910 kJ/mol as listed by the Webbook and by Pedley[76] along with the appearance energy for the $Cr(CO)_3^+$ fragment, we can determine its 298 K heat of formation to be 461.7 kJ/mol. Since the heats of formation of $BzCr(CO)_3^+$ and Bz are known, the $Bz-Cr(CO)_3^+$ bond energy can be determined to be 1.86 eV. This value is 0.12 eV higher than it is in $BzCr^+$, which means that the presence of the CO groups strengthen the Bz−Cr bond.

Conclusions

Threshold photoelectron−photoion coincidence (TPEPICO) spectroscopy and density functional theory have been used to investigate the dissociation kinetics of the benzene chromium tricarbonyl ion, $BzCr(CO)_3^+$. The dissociation of the $BzCr(CO)_3^+$ ion proceeds by the sequential loss of three CO and benzene ligands. By fitting the metastable ion time-of-flight distributions and the breakdown diagram with the statistical RRKM theory, accurate 0 K appearance energies of the four product ions were determined to be 8.33 ± 0.05, 8.93 ± 0.05, 9.97 ± 0.06, and 11.71 ± 0.06 eV, respectively. Combined with the ionization energy of $BzCr(CO)_3$, 7.30 ± 0.05 eV, the ion bond energies for all three Cr^+-CO bonds and the $Bz-Cr^+$ bond were obtained to be 1.03 ± 0.05, 0.60 ± 0.05, 1.04 ± 0.05, and 1.74 ± 0.05 eV, respectively. Using the known heats of formation of the fully dissociated products, benzene, Cr^+, and CO, the heats of formation of $BzCr(CO)_n^+$ ($n = 3\rightarrow0$) are determined to be 365.1 ± 7.7, 579.3 ± 7.7, 752.6 ± 7.0 and 964.7 ± 5.0 kJ/mol, and the heat of formation of $BzCr(CO)_3$ is -341.5 ± 6.0 kJ/mol. Using the IE value of BzCr and the scaled DFT bond energies of $BzCr(CO)_n$ ($n = 3\rightarrow1$), the heats of formation of neutral $BzCr(CO)_2$, BzCrCO, and BzCr were determined to be -9 ± 15, 328 ± 15, and 470.9 ± 6.3 kJ/mol, respectively.

Acknowledgment. We thank Dr. Bálint Sztáray for the use of his program that analyzes the data and the Department of Energy for financial support of this work.

Supporting Information Available: Equilibrium structures of neutral and ionic $BzCr(CO)_n$ ($n = 3\rightarrow0$) and vibrational frequencies used in the simulations (PDF). This material is available free of charge via the Internet at http://pubs.acs.org.

JA012630M

(74) Calhorda, M. J.; Frazao, C. F.; Simoes, J. A. M. *J. Organomet. Chem.* **1984**, *262*, 305−314.
(75) Chen, Y. J.; Liao, C. L.; Ng, C. Y. *J. Chem. Phys.* **1997**, *107*, 4527−4536.
(76) Pedley, J. B.; Rylance, J. *Sussex-NPL Computer Analysed Thermochemical Data: Organic and Organometallic Compounds*; University of Sussex: Sussex, U.K., 1977.